JOP. J Pancreas (Online) 2007; 8(6):725-738.

ORIGINAL ARTICLE

Ultrastructural Islet Study of Early Fibrosis in the Ren2 Rat Model of Hypertension. Emerging Role of the Islet Pancreatic Pericyte-Stellate Cell

Melvin R Hayden[1,2,3], Poorna R Karuparthi[1,3], Javad Habibi[1,2,3,5], Chetan Wasekar[1,3], Guido Lastra[1,2,3,5], Camilla Manrique[1,2,3,5], Sameer Stas[1,2,3,5], James R Sowers[1,2,3,4,5]

Departments of [1]Internal Medicine, [2]Endocrinology Diabetes and Metabolism, [3]Diabetes and Cardiovascular Research Center, [4]Physiology and Pharmacology, [5]Harry S Truman VA Medical Center; University of Missouri School of Medicine. Columbia, MO, USA

ABSTRACT

Context Type 2 diabetes mellitus is a multifactorial disease with polygenic and environmental stressors resulting in multiple metabolic toxicities and islet oxidative stress. We have integrated the role of the islet renin-angiotensin system (RAS) in the pathogenesis of early islet fibrosis utilizing the transgenic (mRen2)27 rodent model of hypertension and tissue RAS overexpression.

Objective The Ren2 pancreatic islet tissue was evaluated with transmission electron microscopy to study both early cellular and extracellular matrix remodeling.

Animals Four 9- to 10-week-old male Ren2 untreated models and four Sprague Dawley sex and age matched controls were used.

Design Ultrastructural study to compare pancreatic islet tissue.

Main outcome measures Only qualitative and observational transmission electron microscopy findings are reported.

Results Major remodeling differences in the Ren2 model were found to be located within the islet exocrine interface, including deposition of early fibrillar-banded collagen (fibrosis) and cellular remodeling of the pericyte suggesting proliferation, migration, hypertrophy and activation as compared to the Sprague Dawley controls.

Conclusion This study points to the possibility of the pericyte cell being one of many contributors to the fibrogenic pool of cells important for peri-islet fibrosis as a result of excess angiotensin II at the local tissue level in the Ren2 model. These findings suggest that the pericyte may be capable of differentiating into the pancreatic stellate cell. This islet ultrastructure study supports the notion that pericyte cells could be the link between islet vascular oxidative stress and peri-islet fibrosis. Pericyte-endothelial-pancreatic stellate cell associations and morphology are discussed.

INTRODUCTION

Type 2 diabetes mellitus (T2DM) has reached pandemic proportions and current predictions are that this trend will increase [1, 2]. Thus, a better understanding of islet renin-angiotensin-aldosterone system (RAAS) mechanisms may help in ascertaining how islet structure and function are involved in the early changes associated with the over-expression of islet tissue RAAS. Therefore, we have chosen to study the transgenic (mRen2)27 control rat model of hypertension

and insulin resistance (due to transfection of the mouse renin gene), which is known to result in the overproduction of local tissue angiotensin II in the heart, kidney, skeletal muscle and presumably the islet [3, 4, 5, 6, 7, 8].

There have been a number of publications regarding the role of an active RAAS in the islet [9, 10, 11, 12, 13, 14, 15]. Additionally, studies have shown that RAAS blockade utilizing angiotensin converting enzyme inhibitor(s) and angiotensin type 1 blocker(s) abrogate islet remodeling changes including fibrosis [9, 10, 11, 12, 13, 14, 15].

Angiotensin II significantly impairs pancreatic islet blood flow in isolated perfused rat pancreata and inhibits insulin release from isolated mouse islets in response to high glucose due to high proinsulin synthesis [10, 16] and both of these abnormalities are improved with RAAS blockade [10, 16]. Angiotensin II is also known to activate the NAD(P)H oxidase enzyme, which results in islet oxidative stress due to the excess production of reactive oxygen species within the islet [17, 18, 19, 20, 21]. The islets have a limited ability to handle oxidative stress making them quite vulnerable to functional and structural remodeling changes [22, 23, 24].

Insulin resistance resulting in compensatory elevated levels of insulin, proinsulin and amylin [18] may activate the local islet RAAS [25, 26] and once depleted hyperglycemia continues RAAS activation, which causes additional damage to these vulnerable islets [18, 27]. RAAS expression is up-regulated in the endocrine pancreas in T2DM and blockade with converting enzyme inhibitors and angiotensin type 1 blockers result in improvement of both islet function and structure in animal models of T2DM.

The purpose of this investigation was to examine the early ultrastructural changes of extracellular matrix remodeling fibrosis and the associated cellular remodeling of these fibrotic changes in the Ren2 model as compared to the Sprague Dawley control model. The finding of pericyte hyperplasia, activation, migration and its close association with early fibrillar-banded collagen in the islet exocrine interface was unexpected. Further, these observational findings support a role for the pericyte as a possible pancreatic stellate cell-myofibroblast precursor in this model of early peri-islet/islet exocrine interface remodeling fibrosis.

MATERIALS AND METHODS

Animals

Four male Ren2 rats (254.8 g mean body weight) and four age-matched male Sprague Dawley control rats (274.0 g mean body weight) were sacrificed at 9.3-10.2 weeks of age.

Determination of Systolic Blood Pressure and Total Body Weight

Restraint conditioning was initiated on the day of initial systolic blood pressure measurement and measured in triplicate, on separate occasions throughout the day, using the tail-cuff method (Student Oscillometric Recorder Harvard Systems Hatternas Instrument Inc., Cary, NC, USA) on the day prior to sacrifice. Total body weights were obtained at time of sacrifice.

Determination of Glucose

Following an overnight fast, blood was collected prior to sacrifice from the tail vein to determine baseline glucose. Glucose levels were determined on whole blood samples using a glucose oxidase method (OneTouch Ultra glucose analyzer; Lifescan, Inc., Milpitas, CA, USA).

Transmission Electron Microscopy (TEM)

Following harvesting, the tail sections of the pancreatic tissue was thinly sliced and placed in primary electron microscopy fixative (2% glutaraldehyde, 2 % paraformaldehyde in 0.1 M Na cacodylate buffer, pH 7.35). A Pelco 3440 Laboratory Microwave Oven (Ted Pella, Inc., Redding, CA, USA) was utilized for secondary fixation, with acetone dehydration and Epon-Spurr's resin infiltration. Specimens were placed on a rocker overnight at room temperature and embedded the

following morning and polymerized at 60°C for 24 hours. A microtome (Ultracut UCT, Leica Microsystems GmbH, Wetzlar, Germany) with a 45 degree diamond knife (Diatome, Biel, Switzerland) was used to prepare 85 nm thin sections. The specimens were then stained with 5% uranyl acetate and Sato's triple lead stain. A transmission electron microscope (1200-EX, Jeol, Ltd., Tokyo, Japan) was utilized to view all pancreatic samples.

Light Microscopic Histological Preparation and Staining

All pancreatic tissues were harvested from the tail region of the pancreas of all rats, immediately fixed in 3% paraformaldehyde, infiltrated and embedded in paraffin.

Picrosirius Red

Picrosirius red specifically stains types I and III collagen and is birefringent when visualized by crossed polarized light. This staining procedure provides a good measure of tissue fibrosis.

Five microns sections were deparaffinized in xylene, rehydrated in ethanol series and HEPES wash buffer. The sections were stained with 0.2% phosphomolybdic acid for two minutes, rinsed in distilled water and counter-stained with picrosirius red (F3BA, saturated picric acid 400 mL, sirius red 0.4 g) for 110 minutes followed by 0.01 N hydrochloric acid treatment for 2 minutes. Then, the sections were dehydrated in reverse ethanol series, cleared, air dried, and mounted with a synthetic mounting media. The slides were observed under a microscope (Eclipse 50i, Nikon, Tokyo, Japan) and the images were captured and analyzed by MetaVue (Boyce Scientific Inc, Gray Summit, MO, USA) by using a cool camera (SNAP cf, Boyce Scientific Inc, Gray Summit, MO, USA).

Alpha Smooth Muscle Actin (alpha-SMA)

Alpha-SMA antibody staining was utilized to specifically detect activation of profibrogenic cells in tissue and has been used to detect microvascular pericytes in systemic sclerosis [28].

Tissue blocks were washed in PBS, suspended in 6.8% sucrose in PBS (pH 7.4), dehydrated in 100% acetone (60 min at 4°C), and embedded in (3 h at 4°C; no. 7022 2224-861; Historesin Plus Leica, Deerfield, IL, USA); alternatively 1 mm^3 cubes were washed in PBS, dehydrated in cold ethanol at -4 to -20°C, embedded in Unicryl® resin (British BioCell, Cardiff, UK), and polymerized by ultraviolet light (48 h at -10 to -20°C). Two-micrometer sections (Microme HM 355, Richard Allen, St. Louis, MO, USA) were stored at 4°C until use; 90-nm Unicryl® sections were picked up onto formvar-coated nickel grids and stored at room temperature until use.

3-Nitrotyrosine

Detecting the presence of 3-nitrotyrosine is an indirect method to evaluate tissue for the presence of excess reactive oxygen species due to oxidation of nitric oxide and the generation of peroxynitrite, which leads to nitration of tyrosine residues of protein in tissues. The cellular production of highly reactive nitrogen species derived from nitric oxide, such as peroxynitrite, nitrogen dioxide and nitryl chloride, leads to the nitration of tyrosine resides in tissue proteins. The extent of protein nitrotyrosine formation provides an index of the production of reactive nitrogen species and potential cell damage over a period of time.

3-nitrotyrosine content was measured as previously described [4]. Briefly, the pancreas sections were deparafinized, rehydrated, and epitopes were retrieved in citrate buffer. Endogenous peroxidases were quenched with 3% H_2O_2 and non-specific binding sites were blocked with avidin, biotin, and protein block (Dako, Carpinteria, CA, USA). The sections were then incubated with 1:200 primary rabbit polyclonal anti-nitrotyrosine antibody (Chemicon, Temecula, CA, USA). Sections were then washed and incubated with secondary antibodies, linked, and labeled with Strepavidin® (Dako, Carpinteria, CA, USA) for 30 min each. After several rinses with distilled water, diaminobenzidine was applied for 10 min. The sections were again rinsed

with distilled water, stained with hematoxylin for 1 min, rehydrated, and mounted with a permanent media.

ETHICS

All animal procedures were approved by the University of Missouri animal care and use committees and housed/harvested in accordance with NIH guidelines.

STATISTICS

Data are reported as mean±SEM and was statistically evaluated using the Student's t-test for independent samples. Differences between experimental results were considered significant if the two-tailed P value was less than 0.05. No quantitation regarding image analysis was undertaken and therefore no statistical data is presented regarding image analysis.

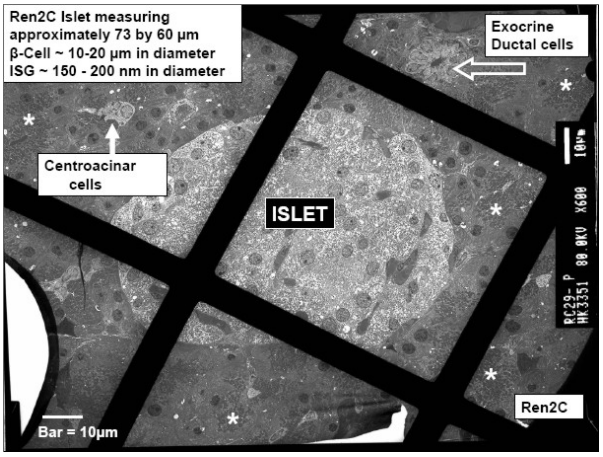

Figure 1. Single islet in Ren2 low power transmission electron microscopy (magnification: 600x; bar: 10 µm). This image demonstrates a well circumscribed, less electron dense and centrally located islet seemingly buried within a sea of exocrine-acinar cells with zymogen granules (*), exocrine duct (open arrow) and centroacinar cells (closed arrow) depicted. Initially, islets appear to be randomly located throughout the pancreas; however, they develop in close proximity and parallel to its vascular supply. This very low power transmission electron microscopy image of the Ren2 model does not demonstrate the peri-islet/islet exocrine interface region with any clarity and is only appreciated at higher magnifications as in subsequent images. This may be one of the reasons why this important anatomical region has been somewhat neglected in the past. The heavy criss-cross bars are the grid bars, which support the specimen and are not usually seen on standard transmission electron microscopy images.
Ren2C: transgenic (mRen2)27 untreated rat model of hypertension

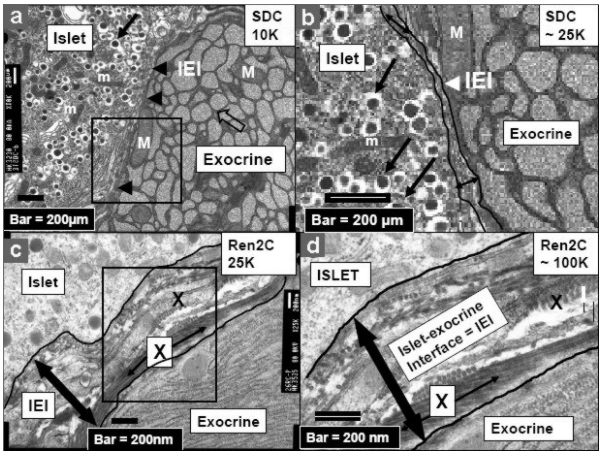

Figure 2. Sprague Dawley *vs.* Ren2 islet exocrine interface comparison. **a.** This transmission electron micrograph (TEM) image depicts the normal islet exocrine interface (IEI) (arrowheads) in the Sprague Dawley control (SDC) rat (magnification: 10K; bar: 200 µm). The islet exocrine interface represents a specialized anatomical area that separates the endocrine-islet and exocrine portions of the pancreas. Note the numerous secretory granules (closed arrow) in the islet portion, tubular mitochondria (m), the lacey endoplasmic reticulum (open arrow) and the much larger-oval shaped mitochondria (M) in the exocrine portion. The boxed in area represents the exploded view in panel b. **b.** The exploded TEM view in this panel demonstrates that the islet exocrine interface still remains a narrow anatomical structure with no evidence of fibrosis in the Sprague Dawley control model (magnification: approximately 25K; bar: 200 µm). **c.** This TEM image of the transgenic Ren2 model (Ren2C) demonstrates islet exocrine interface (double arrow) fibrosis with fibrillar-banded collagen in longitudinal and cross section (X) (magnification: 25K; bar: 200 nm). Note that it is significantly wider than the Sprague Dawley control counterpart in panels a and b. The boxed-in area represents the exploded view of about 100K in panel d. **d.** This panel depicts an exploded view of the boxed-in area of panel c (magnification: approximately 100K; bar: 200 nm). This image allows for a better interpretation of the islet exocrine interface fibrillary collagen (both longitudinal and cross section) representative of fibrosis (X) in the Ren2 model.

RESULTS

The Peri-islet/Islet Exocrine Interface

Low power images less than 10,000 times magnification of the peri-islet region (typical of light microscopy and even low power images by TEM) appear to be quiescent in the

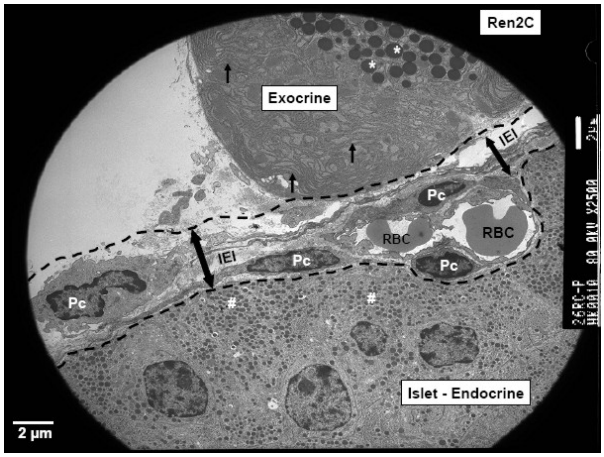

Figure 3. Islet exocrine interface in the Ren2 model with pericyte proliferation, migration and hypertrophy (magnification: 2,500x; bar: 2 µm). This image demonstrates the special anatomical area: the islet exocrine interface (IEI) (double arrows) and is highlighted by bold black dashed lines. This islet exocrine interface contains an anuclear endothelial capillary containing two red blood cells (RBC) with four adjacent pericytes (Pc) in the transgenic Ren2 model (Ren2C) undergoing: proliferation, migration and hypertrophy. In subsequent figures it will be noted that the foot processes demonstrate the presence of actin filaments (Figure 5), and that these cells are activated and demonstrate the presence of alpha-smooth muscle actin (Figure 7cd) and become associated with the formation of fibrillar-banded collagen within the islet exocrine interface (Figure 4cd). Superior to the islet exocrine interface is an exocrine acinar cell containing endoplasmic reticulum (arrows), zymogen granules (asterisks) and inferior to the islet exocrine interface is the endocrine-islet portion containing islet secretory cells and secretory granules (#). Activation of pericyte induce them to proliferate, migrate to sites of tissue damage, increase contractility, phygocytize and to become capable of synthesizing fibrillar-banded collagen representative of islet exocrine interface fibrosis (Figure 4cd).

Sprague Dawley and Ren2 animal models (Figures 1 and 2); however, on higher magnification this anatomical region seems to reflect considerable remodeling changes and important cellular activity as compared to the Sprague Dawley control model (Figure 2). There were no notable observational differences between the Ren2 and Sprague Dawley rats regarding beta-cell apoptosis, beta-cell ultrastructural organelles (mitochondria, endoplasmic reticulum, insulin secretory granules, Golgi apparatus and nuclear contents) or intra-islet fibrosis.

The peri-islet/islet exocrine interface is an important anatomical and functional region between the endocrine and exocrine pancreas, which contains the neurovascular supply including the afferent and efferent vessels (Figure 2) [29]. The islet exocrine interface region allows for communication between the islet and the exocrine pancreas and has been shown to develop significant fibrosis in the Zucker obese model of T2DM as well as T2DM in humans, which is also associated

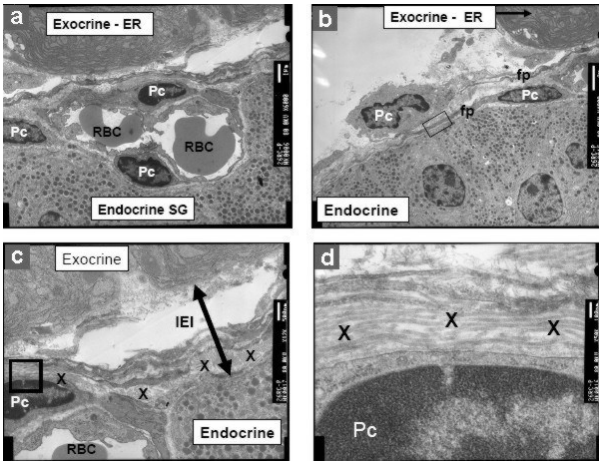

Figure 4. Pericyte proliferation, migration, hypertrophy and collagen synthesis depicting the Ren2 model islets. **a.** This panel represents a higher power view of Figure 3, demonstrating three pericytes (Pc) in close proximity to an islet exocrine interface anuclear endothelial capillary containing two red blood cells (RBC) (magnification: 6K; bar: 1 µm). Sprague Dawley control models have only one pericyte associated with the capillary endothelial cell (Figure 11ab). The presence of multiple pericytes in this Ren2 model supports the notion, morphologically, that these pericytes are undergoing proliferation. **b.** This panel depicts a more hypertrophic pericyte and note the long foot processes (fp) extending from two separate pericytes (magnification: 4K; bar: 2 µm). The boxed-in area is magnified to 60K in Figure 5. **c.** This panel demonstrates a pericyte sitting atop of a capillary containing a red blood cell (RBC) within the islet exocrine interface (IEI) (double arrow) (magnification: 12K; bar: 500 nm). Note the close association of adjacent fibrillar-banded collagen (X). The boxed in section is depicted at higher magnification in panel d. **d.** This panel depicts the boxed in area of the pericyte from panel c at higher magnification (magnification: 50K; bar: 100 nm). This image demonstrates fibrillar-banded collagen (X) being formed adjacent to this pericyte, which suggests the early capability to synthesize collagen in close proximity to the capillary endothelial cell.

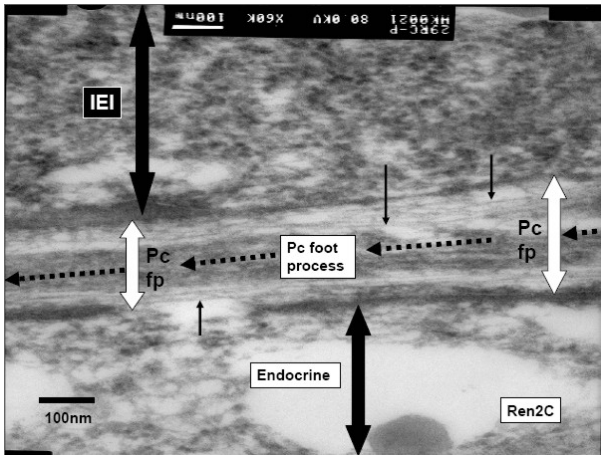

Figure 5. Pericyte foot process with actin filaments. This image of the transgenic Ren2 model (Ren2C) pericyte (Pc) foot process (fp) (white-blocked double arrows) is a higher magnification of the boxed in area of Figure 4b and demonstrates the presence of actin filaments running longitudinally within the foot process (black arrows) (magnification: 60K; bar: 100 nm). Not only will these filaments allow for contraction but also they may aid in the support of migration of the pericyte cell within the islet exocrine interface (IEI), especially when alpha smooth muscle actin gene expression is activated and expressed as in Figure 7. Note that not only is the activated pericyte capable of migration (Figures 3 and 4) but also is associated with the synthesis of banded-fibrillar collagen as in Figure 4cd. The islet exocrine interface superiorly and the endocrine portion inferiorly in this image are demarcated by black-blocked double arrows. The dashed arrows represent the directional extension of the foot process (fp) from the nuclear portion of the pericyte cell.

with islet amyloid deposition both within the islet and this specialized peri-islet - interface location [15, 29, 30].

The presence of fibrillar-banded collagen was eminent in the Ren2 model at the islet exocrine interface but this was not observed in the Sprague Dawley model pancreas (Figure 2). As a result of these findings it was hypothesized that there might exist a morphological change in the islet exocrine interface pericyte, which could possibly be responsible for this fibrillar-banded collagen deposition. It is known that the pericyte can differentiate into multiple cell types including myofibroblasts capable of synthesizing and depositing fibrillar-banded collagen [31, 32, 33]. Subsequently, the decision was made to examine multiple capillaries within islet exocrine interface to evaluate any changes of the pericyte that might support a role for its relationship to the fibrillar-banded collagen and the very early fibrosis observed within the islet exocrine interface.

Novel Pericyte Findings

The novel finding of pericyte proliferation, migration, hypertrophy (Figures 3, 4) was further supported by the finding of actin filaments in pericyte foot processes on higher magnification suggesting activation (Figure 5). Additionally, there was a morphological association of fibrillar-banded collagen with the activated pericyte in the islet exocrine interface of the Ren2 rats at 9-10 weeks of age (Figure 4d). Since the initial submission of this paper, our group has found direct image evidence in the human islet amyloid

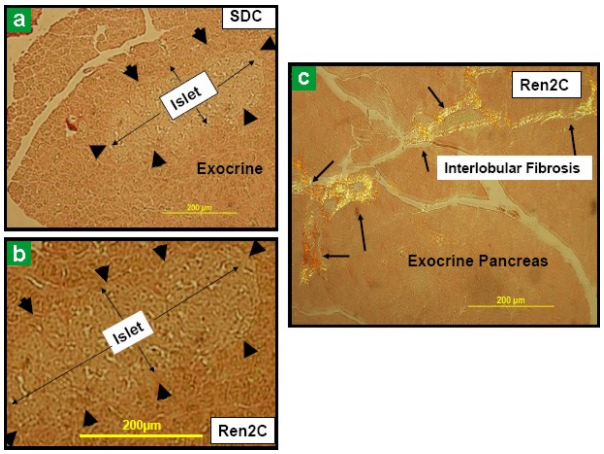

Figure 6. Picrosirius red staining and crossed polarized light. Lack of peri-islet fibrosis and presence of interlobular fibrosis in the Ren2 model. **a.** This panel depicts an islet (arrows) in a sea of exocrine tissue in the Sprague Dawley control. Note there is no peri-islet/islet exocrine interface or interlobular gold colored signal for types I or III collagen with picrosirius red staining and crossed polarized light (arrowheads) (magnification: 20x; bar: 200 µm). **b.** Islet denoted by arrows, demonstrating no gold colored signal for types I or III collagen with picrosirius red staining at the islet exocrine interface (arrowheads) with crossed polarized light in the transgenic Ren2 model (magnification: 40x; bar: 200 µm). **c.** This panel depicts a strong interlobular gold colored signal for types I and III collagen with picrosirius red staining and cross polarized light in the transgenic Ren2 model (arrows). These findings indicate extensive interlobular fibrosis in the Ren2 model of hypertension and insulin resistance (magnification: 20x; bar: 200 µm).

polypeptide rat model of type 2 diabetes mellitus (harboring the human amylin gene) of the pericyte actively extruding banded collagen fibrils from the pericyte (unpublished data). These structural changes within the extracellular matrix of the islet exocrine interface were felt to represent a very early fibrosis and these extracellular matrix and cellular remodeling changes of the pericyte were not noted in the age-matched Sprague Dawley control model. To our knowledge this is the first TEM investigation demonstrating pericyte cellular differentiation of this vascular mural cell into a fibrogenic cell such as the pancreatic stellate cell-myofibroblast in the Ren2 model of early fibrosis, hypertension and insulin resistance.

There was no evidence of peri-islet/interface fibrosis in the Sprague Dawley or Ren2 model utilizing picrosirius red staining and crossed polarized light (Figure 6ab). These picrosirius red findings have also been substantiated by utilizing the Verhoeff Van Gieson staining method for fibrosis (data not shown). These findings support the notion that peri-islet/islet exocrine interface changes of fibrosis occur very early in the Ren2 model and can only be identified utilizing TEM imaging. Importantly, there was no exocrine inter-lobular fibrosis in the Sprague Dawley control model; however, there was a definite increase in the exocrine interlobular extracellular matrix in the Ren2 model (Figure 6c), which was felt to be indicative of exocrine interlobular fibrosis. These remodeling changes may indicate a differential spatial and temporal remodeling within the pancreas of the Ren2 rats, in that, interlobular fibrosis occurs earlier and is initially more robust than peri-islet/interface fibrosis.

Pericyte Activation

The previous observations prompted staining for early fibrotic cellular activation with alpha-smooth muscle actin (alpha-SMA). The Sprague Dawley control model rarely demonstrated signals for alpha-SMA antibody staining and when rarely identified, demonstrated only faint signals in the microvessels of the exocrine pancreas (Figure 7a). In contrast, strong signals were readily observed for alpha-SMA antibody staining in the interlobular areas of the vessels and ducts (Figure 7b) supporting the finding of interlobular fibrosis (Figure 6c). Importantly, there were strong signals present in the microvessels of the peri-islet/interface areas of the Ren2 model (Figure 7cd). These findings suggest that peri-islet microvascular mural cells, pericytes, and ductal cells were activated in the Ren2 model, which contribute to the early peri-islet/islet exocrine interface fibrillar-banded collagen as well as the exocrine interlobular fibrosis noted by TEM (Figures 2cd, 4cd, 6, 10d). We suggest that that this peri-islet/islet exocrine interface

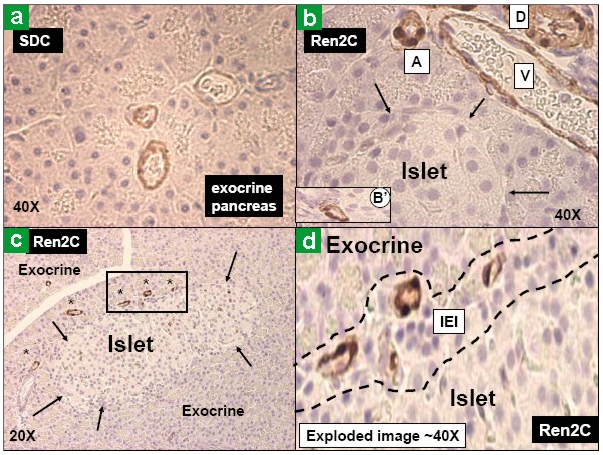

Figure 7. Alpha smooth muscle actin staining. **a.** This panel demonstrates a very faint and rare signal for alpha-smooth muscle actin (alpha-SMA) antibody in the aged-matched Sprague Dawley control model (SDC) exocrine pancreas (magnification: 40x). When rarely found these signals were located in the exocrine microvessels. **b.** This panel depicts a strong signal for alpha-SMA antibody in the duct (D), arteriole (A) and venule (V) in the transgenic Ren2 control model (Ren2C) exocrine pancreas (magnification: 40x). Note there was also a perivascular microvessel signal inferiorly in this islet (arrows) (insert **e.**). **c.** This panel demonstrates an islet (arrows) with a strong signal for alpha-SMA in multiple peri-islet microvessels superiorly (asterisks) in the Ren2 model (magnification: 20x). The boxed-in section is exploded in panel d. **d.** This image is an exploded view of the boxed-in area of panel c and emphasizes the strong signal for alpha-SMA antibody in peri-islet microvessels in the peri-islet/islet exocrine interface (IEI) highlighted by the bold dashed lines (magnification: 20x). Others have used this stain to identify microvascular pericyte [28].

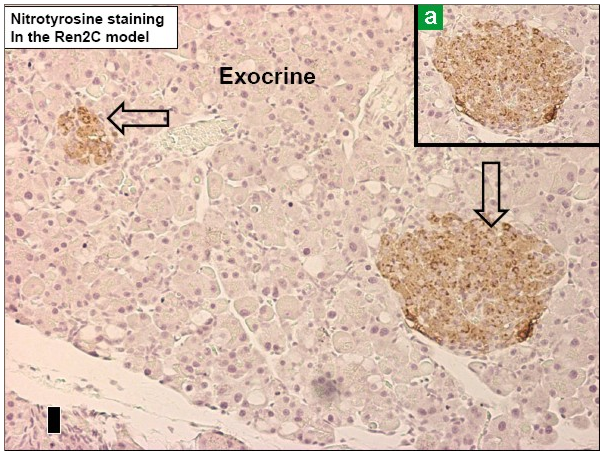

Figure 8. 3-nitrotyrosine staining (magnification: 20x). This image demonstrates the strong diffuse antibody staining for 3-nitrotyrosine in two islets (open arrows) in the transgenicRen2 control model (Ren2C) pancreas indicating intra-islet oxidative stress. Note there is no staining in the exocrine portion of the pancreas as only the islets stained positive for 3-nitrotyrosine. Insert **a.** demonstrates the diffuse intra-islet staining of 3-nitrotyrosine in the Ren2 model. There was no staining for 3-nitrotyrosine in islets or exocrine portion of the age-matched Sprague Dawley control model.

fibrosis would become more pronounced as the Ren2 model ages.

Islet Oxidative Stress

We have previously documented increased tissue organ oxidative stress in the myocardium, renal tubules and glomeruli, skeletal muscle and systemic vasculature of the Ren2 model [3, 4, 5, 6, 7, 8]. Additionally, others have found evidence of increased islet oxidative stress in the Zucker obese animal model of T2DM demonstrating that nitrotyrosine staining was strongly correlated with islet fibrosis and that this was abrogated by treatment with converting enzyme inhibitors and angiotensin type 1 blockers [15]. Recently, we have also documented this finding in a human patient with T2DM at autopsy [29, 30]. Therefore, the staining for the presence of 3-nitrotyrosine seemed imperative in this study and we were able to document a diffuse endocrine intra-islet staining for 3-nitrotyrosine in the Ren2 model, which was not present in the Sprague Dawley control model (Figure 8).

Weights, Blood Pressure and Blood Glucose

The Ren2 animals had lower mean body weights, higher blood pressures and higher blood sugars throughout the study period (Table 1). These findings were comparable to those found by previous investigators who have studied this model [3, 8, 34].

DISCUSSION

The unique finding of early fibrotic changes in the peri-islet/islet exocrine interface in this young Ren2 model of hypertension and insulin resistance [34], with known renin overexpression and most probably an increased local islet tissue RAAS (currently not proven) and increased islet oxidative stress (Figure 8), prompted further speculation.

As a result of the present findings it is currently speculated that the pericyte within the interface region is capable of differentiating into a cell type recently described and termed the pancreatic stellate cell. The pancreatic stellate cell was originally described in the pancreas almost a decade ago [35, 36] and has recently been of topical interest regarding the associated exocrine fibrosis found in various models of pancreatitis [37, 38].

Table 1. Comparison of mean body weight, blood pressure and glucose of Ren2 and Sprague Dawley animal models.

	Animal model		P value[a]
	Ren2	**Sprague Dawley**	
Mean body weight (g)	255±4	274±5	0.025
Initial blood pressure (mmHg)	144.2±1.7	126.2±3.7	0.005
Final blood pressure (mmHg)	160.9±6.8	141.0±0.5	0.027
Blood glucose	162.0±13.4 mg/dL 9.0±0.7 mmol/L	117.0±7.2 mg/dL 6.5±0.4 mmol/L	0.025

[a] Unpaired Student's t-test

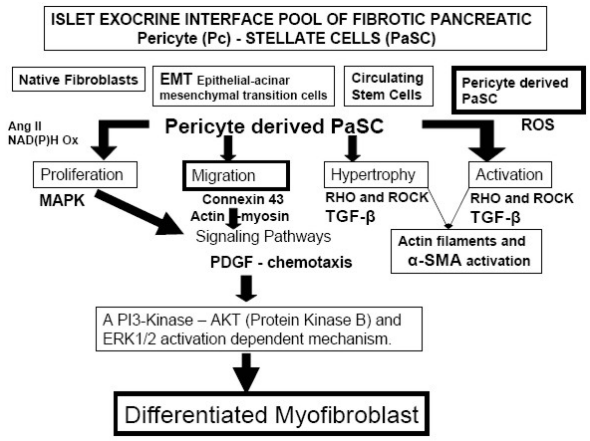

Figure 9. Possible signaling pathways involved in the pericyte-pancreatic stellate cell within the islet exocrine interface. The fibrogenic pool of cells within the islet exocrine interface may arise from various sources including: native fibroblasts, epithelial mesenchymal transition (EMT), circulating stem cells and now the proposed innate proliferating mural vascular cells consisting of pericytes (Pc), which may be capable of differentiating into pancreatic stellate cells (PaSC). It is possible the pericyte derived pancreatic stellate cells may undergo proliferation, migration, hypertrophy and activation as demonstrated with transmission electron microscopy (Figures 3, 4, and 5). The various growth factors and signaling pathways are depicted. The strong signal for alpha-SMA in Figure 7cd further supports the notion that pericyte mural cells may play a significant role in peri-islet fibrosis.
AKT: protein kinase B; ERK: extracellular regulated kinase; G proteins: a class of cell membrane proteins that function as intermediaries between hormone receptors and effector enzymes enabling the cell to regulate its metabolism in response to hormonal changes; MAPK: mitogen activated kinase; Pc: pericyte; PDGF: platelet derived growth factor; PI3-kinase: phosphatidylinositol 3-kinase pathway; RHO: a member of the RAS superfamily of small G proteins; ROCK: RHO kinase; TGF-beta: transforming growth factor beta

As a result of our current observational findings we propose that the pool of fibrogenic pancreatic stellate cells includes not only the native fibroblasts, circulating stem cells, epithelial-acinar mesenchymal transition cells but also the differentiated microvascular pericyte. Some of the possible signaling pathways involved with the proliferation, migration, hypertrophy and activation of the pericyte-pancreatic stellate cell are presented (Figure 9).

The normal islet matrix capsule in the Sprague Dawley control model is somewhat reminiscent and morphologically similar in

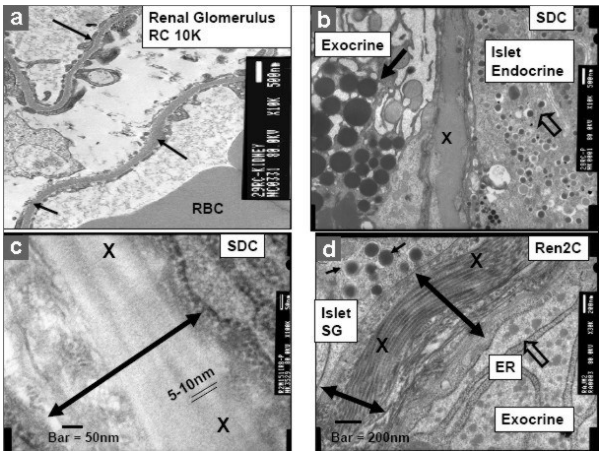

Figure 10. Islet matrix capsule. **a.** This panel reveals a renal glomerulus of a transgenic Ren2 control model (Ren2C) kidney (magnification: 10K; bar: 500 nm). This image depicts the renal glomerular basement membrane (arrows) and serves to demonstrate the morphological similarity to the islet matrix capsule. This matrix is depicted in panel b. **b.** This panel depicts the islet exocrine interface matrix capsule (X) between the endocrine and exocrine portions of the pancreas in the Sprague Dawley control model (SDC) (magnification: 10K; bar: 500 nm). This type of matrix capsule is occasionally observed in the Sprague Dawley control model in addition to the near absence of matrix material in figure 2a; however, one never observes accumulation of fibrillar-banded collagen in the Sprague Dawley control model. Exocrine zymogen granules (arrow) and endocrine secretory granules (open arrow) are depicted. **c.** This panel demonstrates a higher magnification of the islet matrix capsule (double arrow) (magnification: 100K; bar: 50 nm). Type VI collagen is known to be the most abundant collagen type in the islet matrix capsule in rodents and humans; however, it is not possible to be certain that we are visualizing type VI collagen (X) in this view, as there is only very faint banding at approximately 5-10 nm noted. Other matrix contents in the islet-exocrine matrix capsule are known to contain collagens type IV and V (non fibrillar), decorin, laminin, enactin, proteoglycans and glycosaminoglycans (amorphous). **d.** This image depicts the islet exocrine interface (double arrows) separating the islet on the upper left with secretory granules (SG) (arrows) and the exocrine portion of the pancreas on the lower right containing endoplasmic reticulum (ER) (open arrow) (magnification: 30K; bar: 200 nm). Note the banded-fibrillar collagen longitudinally within the islet exocrine interface (X). This was a typical finding in the Ren2 model and was never observed in the Sprague Dawley control model.

appearance to the glomerular basement membrane when visualized at lower TEM magnification (Figure 10ab); however, when viewed at higher magnification there is a suggestion of very faint banding at approximately 10 nanometers (Figure 10c). This matrix capsule is known to contain predominately type VI collagen as compared to types I, II or IV collagen [39, 40]. This is in contrast to the findings in the Ren2 model, in that; the Ren2 rats frequently demonstrated orderly fibrillar-banded collagen typical of very early fibrosis at the islet exocrine interface of Ren2 rat islets (Figures 2cd; 10d).

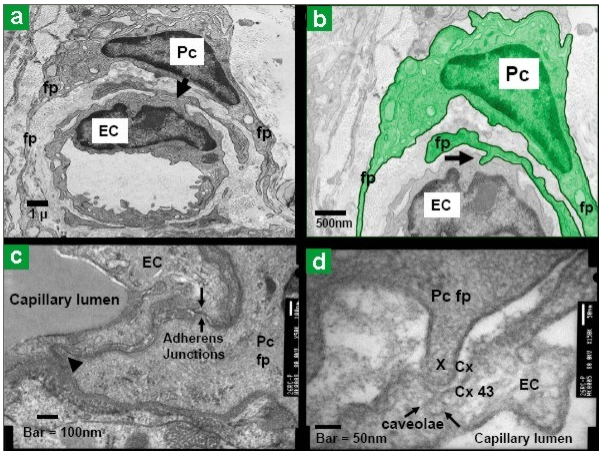

Figure 11. Morphology of pericyte-endothelial interaction. **a.** This panel depicts a normal pericyte (Pc) sitting atop an endothelial cell (EC) of a capillary within the islet of a Sprague Dawley control rodent model (SDC) (magnification: 5K; bar: 1µm). One will note the foot process (fp) surround and envelop the endothelial cell as if embracing it. Note the interdigitation and the sharing of the basement membrane typical of pericyte-endothelial cell interactions (arrow). **b.** This panel depicts the same Sprague Dawley control model pericyte (highlighted) of panel a at a higher magnification and demonstrates one of the intricate attachments between the pericyte and the endothelial cell, termed peg-sockets (arrow) (magnification: 15K; bar: 500 nm). This allows for not only a physical attachment but also crosstalk-communication between these two cells. The peg sockets contain tight, gap (connexins 37, 40, and 43) and adherens junctions (N-cadherins). **c.** This image depicts both a peg-socket (arrowhead) and an adherens junction (arrows) between the pericyte and the endothelial cell of an islet exocrine interface capillary in the Ren2 model where a pericyte foot process (fp) joins the endothelial cell (magnification: 50K; bar: 100 nm). **d.** This high power image demonstrates a less physically well developed peg-socket in the Ren2 model from a pericyte foot process (superiorly) (X) invaginating into the endothelial cell (inferiorly) at the islet exocrine interface (magnification: 150K; bar: 50 nm). Note the caveolae (arrows) in the endothelial cell just below the invaginating peg (X).

The Emerging Role of the Pericyte-Pancreatic Stellate Cell in Early Peri-Islet Fibrosis

The potential role of the pericyte as a pancreatic stellate cell-myofibroblast precursor in the Ren2 model of early peri-islet/interface fibrosis merits further discussion. First, a number of studies have highlighted the *in vivo* capacity of the pericyte to act as mesenchymal precursor cells [34, 41, 42, 43, 44, 45, 46]. Second, during liver and renal fibrosis, resident pericyte cells have been shown to differentiate into myofibroblasts [41, 46]. The objective of our study was to investigate both early cellular and extracellular matrix remodeling and we unexpectedly found the possible relationship of the pericyte being a precursor to the pancreatic stellate cell-myofibroblast cell-lines capable of synthesizing fibrillar-banded collagen within the anatomical region of the peri-islet/islet exocrine interface. This evidence is now even stronger, since our group has recently observed images demonstrating islet exocrine interface pericytes actively extruding banded collagen fibrils in the human islet amyloid polypeptide rat model of type 2 diabetes mellitus (unpublished data).

The pericyte is a mesenchymal, pluripotent, ubiquitous, requisite and vascular smooth muscle-like mural cell found throughout the microvasculature (Figure 11a). It plays an important role as a regulator of stabilization, vascular development, maturation and microvessel physiological repair and pathological cellular and extracellular remodeling processes. It is located immediately adjacent to the endothelial cell where it shares physical connections referred to as peg sockets and adherens junctions (Figure 11bcd) [30, 47, 48, 49]. In addition to the cell-cell physical connections the pericyte has cell-cell molecular connections termed connexin(s) with connexin 43 being the

primary connexin associated with pericyte/endothelial cell interactions. These connexins allow for the transfer of small molecules such as calcium ions, sodium ions, potassium ions and adenosine triphosphate,

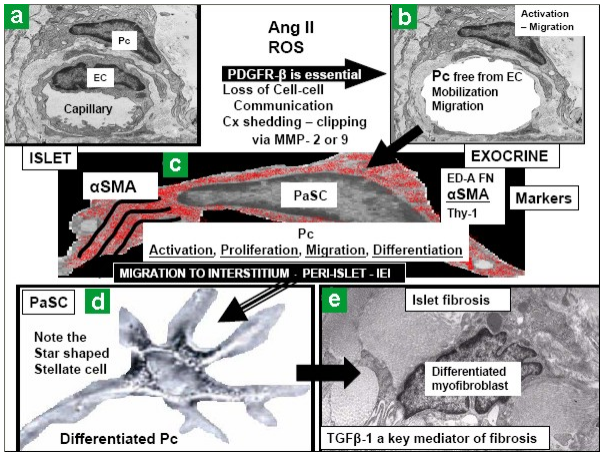

Figure 12. From pericyte to pancreatic stellate cell to the myofibroblast and fibrosis. This figure utilizes transmission electron microscopy images in a cartoon fashion to demonstrate how the pericyte (Pc) may become clipped or freed from the mural endothelial cell (EC) of the capillary due to excess intra- and peri-islet RAS, angiotensin II and reactive oxygen species activity in this transgenic Ren2 model (Ren2C) under investigation. **a.** Loss of cell-cell communication as a result of connexin shedding or clipping by matrix metalloproteinase(s) (MMP) induced by excessive reactive oxygen species allowing the pericyte to be freed and migrate from its native pericapillary connections to the endothelial cell. It is noted in the directing arrow that platelet derived growth factor beta (PDGF-beta) has been determined to be essential for this pericyte activation. **b.** The pericyte then becomes mobilized and activated with the formation of alpha-smooth muscle actin (alpha-SMA) and is free to proliferate, migrate and differentiate. **c.** The pericyte may be considered a pancreatic stellate cell at this stage. The markers for pancreatic stellate cell activation include: extra domain A of fibronectin (ED-A Fn), alpha-SMA and thymus cell antigen-1 (Thy-1). **d.** This portrayed and hand sketched image represents the star shaped pancreatic stellate cell. **e.** This panel depicts a classic differentiated myofibroblast cell surrounded by whorls of collagen deep within the peri-islet tissue fibrosis of a Zucker obese model of type 2 diabetes mellitus with known intra- and peri-islet fibrosis. It is important to note that transforming growth factor beta-1 (TGFbeta-1) is a key mediator of islet fibrosis. In the Ren2 model of hypertension and insulin resistance it is important to note that there is not only the early fibrillar-banded collagen of fibrosis at the peri-islet/islet exocrine interface (Figures 3, 4, 5, and 10d) but also the interlobular exocrine fibrosis as noted in Figure 6c.

which are necessary for maintenance of cellular homeostasis including proliferation and differentiation [50]. The pericytes numerous foot processes-pseudopods literally embrace or envelop the endothelium (Figure 11ab) and are also capable of reaching out long distances to more distant endothelial cells or its surrounding matrix (Figures 3, 4, 11). It provides protection and physical support to the endothelium and nourishes the endothelial cell [50, 51, 52]. The pericyte has previously been referred to as the guardian angel of the endothelial cell and will literally lay down its life for the endothelial cell [51, 52]. Once this pericyte loss (due to apoptosis or necrosis) occurs in retinas of diabetic models, the endothelial cell becomes extremely vulnerable to the effects of reactive oxygen species/oxidative stress and glucotoxicity resulting in acellular capillaries and microaneurysms [50].

Recently, due to findings in genetic mouse models, failure of pericyte-endothelial cell interactions have been associated with numerous human pathological conditions including angiogenesis, diabetic micro-angiopathy, vascular calcification and resulted in severe or even lethal cardiovascular defects [32, 51]. Since the pericyte is pluripotent, plastic and capable of proliferation, migration, hypertrophy and activation into a fibrogenic cell (Figure 12), could the pericyte possibly be the clevis or linchpin that links microvascular damage and endothelial dysfunction to pancreatic peri-islet/islet exocrine interface and interlobular exocrine fibrosis?

In conclusion, the peri-islet/islet exocrine interface findings are preliminary, qualitative and observational; however, they are quite suggestive for supporting the role of excess local tissue islet renin, angiotensin II and oxidative stress being responsible for the very early fibrotic changes found in this young Ren2 model of hypertension and insulin resistance. Further, these observational findings support the role of the pericyte as a possible pancreatic stellate cell-myofibroblast precursor in this model of early peri-islet/islet interface remodeling fibrosis.

Hopefully, these findings will support a proof of concept and stimulate more in-depth investigations of T2DM animal models as well as T2DM islet and pancreatic tissue in humans. This model with its islet and peri-islet cellular and extracellular remodeling fibrosis would provide an excellent model to evaluate renin-angiotensin-aldosterone blockade and direct renin inhibition to see if they could abrogate these very early islet remodeling changes in the Ren2 model. Further utilization of light microscopy with special staining and lighting to help confirm these TEM findings and the use of different treatment modalities may elucidate the role of excess islet and pancreatic angiotensin II and the associated role of the pericyte-pancreatic stellate cell not only in the peri-islet/islet exocrine interface but also in the interlobular exocrine pancreatic regions. Additionally, we feel our observational findings may help to better understand the development of T2DM in those patients with chronic pancreatitis.

Received June 4th, 2007 - Accepted August 10th, 2007

Keywords Angiotensin II; Insulin Resistance; NADPH Oxidase; Oxidative Stress; Reactive Oxygen Species; Renin

Abbreviations Alpha-SMA: alpha smooth muscle actin; T2DM: type 2 diabetes mellitus; RAAS: renin-angiotensin-aldosterone system; TEM: transmission electron microscopy

Acknowledgment This research was supported by the investigator initiated grants NIH (R01 HL73101-01A1), the Veterans Affairs Merit System (0018) grant and Novartis Pharmaceuticals. Male transgenic Ren2 rats and male Sprague-Dawley controls were kindly provided by Dr. Carlos M. Ferrario, Wake Forest University School of Medicine, Winston-Salem, North Carolina through the Transgenic Core Facility supported in part by NIH grant HL-51952. The authors would like to acknowledge the Electron Microscopic Core Center at the University of Missouri, Columbia, Missouri for their excellent help and tissue preparation of animal samples for viewing.

Conflict of interest The authors have no potential conflicts of interest

Correspondence
Melvin R Hayden
Department of Internal Medicine
University of Missouri School of Medicine
D109 HSC Diabetes Center
One Hospital Drive
Columbia, Missouri 65212
USA
Phone: +1-573.346.3019
Fax: +1-573.346.0152
E-mail: mrh29@usmo.com

Document URL: http://www.joplink.net/prev/200711/03.html

References

1. Amos AF, McCarty DJ, Zimmet P. The rising global burden of diabetes and its complications: estimates and projections to the year 2010. Diabet Med 1997; 14:S1-85. [PMID 9450510]

2. Zimmet O. The burden of type 2 diabetes: are we doing enough? Diabetes Metab 2003; 29:6S9-18. [PMID 14502096]

3. Whaley-Connell A, Govindarajan G, Habibi J, Hayden MR, Cooper SA, Wei Y, et al. Angiotensin-II mediated oxidative stress promotes myocardial tissue remodeling in the rransgenic TG (mRen2) 27 Ren2 Rat. Am J Physiol Endocrinol Metab 2007; 293:E355-63. [PMID 17440033]

4. Habibi J, Whaley-Connell A, Qazi MA, Hayden MR, Cooper SA, Tramontano A, et al. Rosuvastatin, a HMG-CoA Reductase Inhibitor, Decreases Cardiac Oxidative Stress and Remodeling in Ren2 Transgenic Rats. Endocrinology 2007; 148:2181-8. [PMID 17317778]

5. Stas S, Whaley-Connell A, Habibi J, Appesh L, Hayden MR, Karuparthi PR, et al. Mineralocorticoid receptor blockade attenuates chronic angiotensin-II overexpression stimulation of NADPH oxidase and cardiac remodeling. Endocrinology 2007; 148:3773-80. [PMID 17494996]

6. Hayden MR, Chowdhury NA, Cooper SA, Whaley-Connell A, Habibi J, Witte L, et al. Proximal tubule microvilli remodeling and albuminuria in the Ren2 transgenic rat. Am J Physiol Renal Physiol 2007; 292:F861-67. [PMID 17032939]

7. Whaley-Connell AT, Chowdhury NA, Hayden MR, Stump CS, Habibi J, Wiedmeyer CE, et al. Oxidative stress and glomerular filtration barrier

injury: role of the renin-angiotensin system in the Ren2 transgenic rat. Am J Physiol Renal Physiol 2006; 291:F1308-14. [PMID 16788142]

8. Wei Y, Sowers JR, Nistala R, Gong H, Uptergrove GM, Clark SE, et al. Angiotensin II-induced NADPH oxidase activation impairs insulin signaling in skeletal muscle cells. J Biol Chem 2006; 281:35137-46. [PMID 16982630]

9. Carlsson PO. The renin-angiotensin system in the endocrine pancreas. JOP. J Pancreas (Online) 2001; 2:26-32. [PMID 11862019]

10. Lau T, Carlsson PO, Leung PS. Evidence for a local angiotensin system and dose-dependent inhibition of glucose-stimulated insulin release by angiotensin II in isolated pancreatic islets. Diabetologia 2004; 47:240-48. [PMID 14722647]

11. Leung PS. Pancreatic renin-angiotensin system: a novel target for the potential treatment of pancreatic diseases? JOP. J Pancreas (Online) 2003; 4:89-91. [PMID 12629265]

12. Leung PS, Carlsson PO. Tissue renin-angiotensin system: its expression, localization, regulation and potential role in the pancreas. J Mol Endocrinol 2001; 26:155-64. [PMID 11432370]

13. Leung PS, Chappell MC. A local pancreatic renin-angiotensin system: endocrine and exocrine roles. Int J Biochem Cell Biol 2003; 35:838-46. [PMID 12676170]

14. Tahmasebi M, Puddefoot JR, Inwang ER, Vinson GP. The tissue renin-angiotensin system in human pancreas. J Endocrinol 1999; 161:317-22. [PMID 10320830]

15. Tikellis C, Wookey PJ, Candido R, Andrikopoulos S, Thomas MC, Cooper ME. Improved islet morphology after blockade of the renin- angiotensin system in the ZDF rat. Diabetes 2004; 53:989-97. [PMID 15047614]

16. Kampf C, Lau T, Olsson R, Leung PS, Carlsson PO. Angiotensin II type 1 receptor inhibition markedly improves the blood perfusion, oxygen tension and first phase of glucose-stimulated insulin secretion in revascularised syngeneic mouse islet grafts. Diabetologia 2005; 48:1159-67. [PMID 15877216]

17. Griendling KK, Minieri CA, Ollerenshaw JC, Alexander RW. Angiotensin II stimulates NADH and NADPH oxidase activity in cultured vascular smooth muscle cells. Circ Res 1994; 74:1141-8. [PMID 8187280]

18. Hayden MR, Sowers JR. Hypertension in type 2 diabetes mellitus. Insulin 2006; 1:22-37.

19. Hayden MR, Stump C, Sowers JR. Organ involvement in cardiometabolic syndrome. J Cardiometab Synd 2006; 1:16-24. [PMID 17675904]

20. Lastra-Gonzalez G, Manrique CM, Govindarajan G, Whaley-Connell A, Sowers JR. Insights into the emerging cardiometabolic prevention and management of diabetes mellitus. Expert Opin Pharmacother 2005; 6:2209-21. [PMID 16218882]

21. Sowers JR. Hypertension, angiotensin II and oxidative stress. N Engl J Med 2002; 346:1999-2001. [PMID 12075063]

22. Hayden MR, Tyagi SC. Islet redox stress: the manifold toxicities of insulin resistance, metabolic syndrome and amylin derived islet amyloid in type 2 diabetes mellitus. JOP. J Pancreas (Online) 2002; 3:86-108. [PMID 12110767]

23. Sakurai K, Katoh M, Someno K, Fujimoto Y. Apoptosis and mitochondrial damage in INS-1 cells treated with alloxan. Biol Pharm Bull 2001; 24:876-82. [PMID 11510477]

24. Turk J, Corbett JA, Ramanadham S, Bohrer A, McDaniel ML. Biochemical evidence for nitric oxide formation from streptozotocin in isolated pancreatic islet. Biochem Biophys Res Commun 1993; 197:1458-64. [PMID 7904159]

25. Cooper ME, McNally PG, Phillips PA, Johnston CI. Amylin stimulates plasma renin concentrations in humans. Hypertension 1995; 26:460-64. [PMID 7649582]

26. Ikeda T, Iwata K, Ochi H. Effect of insulin, proinsulin, and amylin on renin release from perfused rat kidney. Metabolism 2001; 50:763-66. [PMID 11436178]

27. Leung PS. The physiology of a local renin-angiotensin system in the pancreas. J Physiol 2007; 580:31-7. [PMID 17257271]

28. Rajkumar VS, Howell K, Csiszar K, Denton CP, Black CM, Abraham DJ. Shared expression of phenotypic markers in systemic sclerosis indicates a convergence of pericytes and fibroblasts to a myofibroblast lineage in fibrosis. Arthritis Res Ther 2005; 7:R1113-23. [PMID 16207328]

29. Hayden MR, Sowers JR. Isletopathy in type 2 diabetes mellitus: implications of islet RAS, islet fibrosis, islet amyloid, remodeling and oxidative stress. Antioxid Redox Signal 2007; 9:891-910. [PMID 17516840]

30. Hayden MR. Islet amyloid and fibrosis in the cardiometabolic syndrome and type 2 diabetes mellitus. J Cardiometab Syndr 2007; 2:70-5. [PMID 17684452]

31. Collett GD, Canfield AE. Angiogenesis and pericytes in the initiation of ectopic calcification. Circ Res 2005; 96:930-38. [PMID 15890980]

32. Armulik A, Abramsson A, Betsholtz C. Endothelial/pericyte interactions. Circ Res 2005; 97:512-23. [PMID 16166562]

33. Carlile MJ, Sturrock MG, Chisholm DM, Ogden GR, Schor AM. The presence of pericytes and transitional cells in the vasculature of the human dental pulp: an ultrastructural study. Histochem J 2000; 32:239-45. [PMID 10872889]

34. Blendea MC, Jacobs D, Stump CS, McFarlane SI, Ogrin C, Bahtyiar G, et al. Abrogation of oxidative stress improves insulin sensitivity in the Ren-2 rat model of tissue angiotensin II overexpression. Am J Physiol Endocrinol Metab 2005; 288:E353-59. [PMID 15494608]

35. Apte MV, Haber PS, Applegate TL, Norton ID, McCaughan GW, Korsten MA, et al. Periacinar stellate shaped cells in rat pancreas: identification, isolation, and culture. Gut 1998; 43:128-33. [PMID 9771417]

36. Bachem MG, Schneider E, Gross H, Weidenbach H, Schmid RM, et al. Identification, culture, and characterization of pancreatic stellate cells in rats and humans. Gastroenterology 1998; 115:421-32. [PMID 9679048]

37. Omary MB, Lugea A, Lowe AW, Pandol SJ. The pancreatic stellate cell: a star on the rise in pancreatic diseases. J Clin Invest 2007; 117:50-9. [PMID 17200706]

38. Pezzilli R. Pancreatic stellate cells and chronic alcoholic pancreatitis. JOP. J Pancreas (Online) 2007; 8:254-7. [PMID 17356252]

39. White SA, Hughes DP, Contractor HH, London NJ. An investigation into the distribution of different collagen types within adult and juvenile porcine pancreata. J Mol Med 1999; 77:79-82. [PMID 9930933]

40. Hughes SJ, Clark A, McShane P, Contractor HH, Gray DW, Johnson PR. Characterisation of collagen VI within the islet-exocrine interface of the human pancreas: implications for clinical islet isolation? Transplantation 2006; 81:423-26. [PMID 16477230]

41. Schmitt-Graff A, Kruger S, Bochard F, Gabbiani G, Denk H. Modulation of alpha smooth muscle actin and desmin expression in perisinusoidal cells of normal and diseased human livers. Am J Pathol 1991; 138:1233-42. [PMID 2024709]

42. Doherty MJ, Ashton BA, Walsh S, Beresford JN, Grant ME, Canfield AE. Vascular pericytes express osteogenic potential in vitro and in vivo. J Bone Miner Res 1998; 13:828-38. [PMID 9610747]

43. Ivarsson M, Sundberg C, Farrokhnia N, Pertoft H, Rubin K, Gerdin B. Recruitment of type I collagen producing cells from the microvasculature in vitro. Exp Cell Res 1996; 229:336-49. [PMID 8986617]

44. Sundberg C, Ivarsson M, Gerdin B, Rubin K. Pericytes as collagen-producing cells in excessive dermal scarring. Lab Invest 1996; 74:452-66. [PMID 8780163]

45. Richardson RL, Hausman GJ, Campion DR. Response of pericytes to thermal lesion in the inguinal fat pad of 10-day-old rats. Acta Anat (Basel) 1982; 114:41-57. [PMID 7148377]

46. Hattori M, Horita S, Yoshioka T, Yamaguchi Y, Kawaguchi H, Ito K. Mesangial phenotypic changes associated with cellular lesions in primary focal segmental glomerulosclerosis. Am J Kidney Dis 1997; 30:632-38. [PMID 9370177]

47. Allt G, Lawrenson JG. Pericytes: cell biology and pathology. Cells Tissues Organs 2001; 169:1-11. [PMID 11340256]

48. Sims DE. The pericyte. A review. Tissue Cell 1986; 18:153-74. [PMID 3085281]

49. Shepro D, Morel NM. Pericyte physiology. FASEB J 1993; 7:1031-8. [PMID 8370472]

50. Li AF, Sato T, Haimovici R, Okamoto T, Roy S. High glucose alters connexin 43 expression and gap junction intercellular communication activity in retinal pericytes. Invest Ophthalmol Vis Sci 2003; 44:5376-82. [PMID 14638741]

51. Hayden MR, Tyagi SC, Kolb L, Sowers JR, Khanna R. Vascular ossification-calcification in metabolic syndrome, type 2 diabetes mellitus, chronic kidney disease, and calciphylaxis-calcific uremic arteriolopathy: the emerging role of sodium thiosulfate. Cardiovasc Diabetol 2005; 4:4. [PMID 15777477]

52. Hayden MR, Sowers JR, Tyagi SC. The central role of vascular extracellular matrix and basement membrane remodeling in metabolic syndrome and type 2 diabetes: the matrix preloaded. Cardiovasc Diabetol 2005; 4:9. [PMID 15985157]